[BMIm][Fe(OTf)$_3$], [BMIm][Mn(OTf)$_3$], [BMIm][Li(OTf)$_2$] – Three One-dimensional Infinite Coordination Polymers

Silke Wolf, Yanhua Lan, Annie Powell, and Claus Feldmann

Institut für Anorganische Chemie, Karlsruhe Institute of Technology (KIT), Engesserstraße 15, D-76131 Karlsruhe, Germany

Reprint requests to Prof. Dr. C. Feldmann. Tel.: ++49-721-60842855.
E-mail: claus.feldmann@kit.edu

Z. Naturforsch. **2013**, *68b*, 3 – 9 / DOI: 10.5560/ZNB.2013-2233
Received September 5, 2012

By heating of $FeCl_2$ and $MnCl_2$ in the ionic liquid [BMIm][OTf] (BMIm: 1-butyl-3-methylimidazolium, OTf: trifluoromethanesulfonate), the compounds [BMIm][M(OTf)$_3$] (M: Fe^{+II}, Mn^{+II}) have been obtained as colorless crystals. Similarly, [BMIm][Li(OTf)$_2$] was synthesized by heating of LiCl in [BMIm][OTf]. While the crystal quality of the [BMIm][M(OTf)$_3$] (M: Fe^{+II}, Mn^{+II}) products thus obtained is low, mild oxidation of $Fe(CO)_5$ or $Mn_2(CO)_{10}$ with GeI_4 applied as an alternative in the same ionic liquid allowed a slow growth of well-formed, needle-shaped crystals. According to X-ray structure analysis based on single crystals, [BMIm][M(OTf)$_3$] (M: Fe^{+II}, Mn^{+II}) crystals are monoclinic, and [BMIm][Li(OTf)$_2$] crystals are triclinic. All compounds form infinite $^1_\infty$[M(OTf)$_3$] (M = Fe, Mn) and $^1_\infty$[Li(OTf)$_2$] chains. The compounds have further been characterized by FT-IR spectroscopy, energy-dispersive X-ray analysis (EDX), differential thermal analysis (DTA), thermogravimetry (TG), and magnetic measurements.

Key words: Coordination Polymer, Infinite Chain, Triflate, Ionic Liquid, Crystal Structure, Manganese, Iron, Lithium

Introduction

Ionic liquids have become highly relevant to chemical synthesis, including the preparation of compounds and materials such as metal-organic coordination complexes, metal-organic frameworks, zeolites, or nanoparticles [1 – 4]. Recently, imidazolium-based ionic liquids have received specific interest in inorganic synthesis, due to their excellent redox stability and their good solvent properties for many inorganic compounds [5 – 7]. Depending on the properties of the counterion, several coordination complexes and coordination polymers could already be obtained [1 – 3, 5 – 7]. Quite often unique coordinative bonding and/or structural building units are observed for compounds prepared in ionic liquids. This is due to the non-coordinating properties of some ionic liquids, favoring a coordination of ligands that is typically not observed in the presence of conventional, coordinating solvents (*e. g.*, alcohols, amines).

Coordination complexes with the – in principle – weakly coordinating $[OTf]^-$ or $[NTf_2]^-$ anions were recently presented by Mudring and coworkers. The octanuclear europium cluster $[BMPyr]_6[Eu_8(\mu_4\text{-}O)(\mu_3\text{-}OH)_{12}(\mu_2\text{-}OTf)_{14}(\mu_1\text{-}Tf)_2](HOTf)_{1.5}$ was synthesized in the ionic liquid [BMPyr][OTf] (BMPyr: butylmethylpyrrolidinium, OTf: trifluoromethanesulfonate) [8]. This polynuclear complex is surrounded by a total of sixteen triflate anions, of which fourteen coordinate as μ_2-ligands *via* corner-sharing of two oxygen atoms of the europium-centered polyhedron. The two remaining triflate anions coordinate as μ_1-ligands. In addition, a series of compounds with the composition $[MPPyr]_x[AE(NTf_2)_y]$ (*AE*: alkaline earth metal; $x = 1, 2$; $y = 3, 4$) were obtained under similar conditions [9]. Here, $[MPPyr]_2[AE(NTf_2)_4]$ (*AE*: Ca, Sr) exhibits separated $[AE(NTf_2)_4]^{2-}$ complex anions. As expected, $[OTf]^-$ or $[NTf_2]^-$ do not coordinate the metal center in the presence of more strongly coordinating ligands. For example, $[Mn_4(bet)_{10}(H_2O)_4][Tf_2N]_8$ with a linear $[Mn_4(bet)_{10}(H_2O)_4]^+$ cationic complex (bet: Me_3NCH_2COO, betaine) and $[Ni_5(bet)_{12}(H_2O)_6][Tf_2N]_{10}$ with a chain-like $[Ni_5(bet)_{12}(H_2O)_6]^+$ cation contain $[NTf_2]^-$

only as a non-coordinating anion [10]. There are only few reports on complexes comprising $[OTf]^-$ or $[NTf_2]^-$ as a bidentate bridging ligand. Thus, [MPPyr][$Ba(NTf_2)_3$] contains infinite $^1_\infty[Ba(NTf_2)_3]^-$ chains [9]. Moreover, alkali and alkaline earth metal triflates as well as silver triflate are known to exhibit $[OTf]^-$ as a bridging ligand in layers [11 – 14].

As part of our studies regarding the potential of ionic liquids in inorganic synthesis [15, 16], we obtained the new coordination compounds [BMIm][$Fe(OTf)_3$], [BMIm][$Mn(OTf)_3$] and [BMIm][$Li(OTf)_2$]. The title compounds were prepared by simple heating of $FeCl_2$, $MnCl_2$ and LiCl in [BMIm][OTf] as the ionic liquids (BMIm: 1-butyl-3-methylimidazolium). Well-shaped crystals of [BMIm][$M(OTf)_3$] (M: Fe^{+II}, Mn^{+II}) were alternatively obtained by mild oxidation of $Fe(CO)_5$ or $Mn_2(CO)_{10}$ with GeI_4 in the respective ionic liquid. All compounds contain infinite $^1_\infty[M(OTf)_3]$ (M: Fe, Mn) or $^1_\infty[M(OTf)_2]$ chains (M: Li), in which iron/manganese and lithium are coordinated by six and four $[OTf]^-$ anions, respectively, which serve as bidentate bridging ligands.

Results and Discussion

For optimal crystal growth, the compounds [BMIm][$M(OTf)_3$] (M: Fe, Mn) were prepared by mild oxidation of $Fe(CO)_5$ or $Mn_2(CO)_{10}$ with GeI_4 in [BMIm][OTf] as the ionic liquid. During the reaction, $Fe^{\pm0}/Mn^{\pm0}$ (in $Fe(CO)_5/Mn_2(CO)_{10}$) were oxidized according to the following equation to Fe^{+II}/Mn^{+II} ([BMIm][$M^{+II}(OTf)_3$], [BMIm][$Mn(OTf)_3$]) whereas Ge^{+IV} (GeI_4) was reduced to $Ge^{\pm0}$:

$$2\,Fe(CO)_5 + GeI_4 \rightarrow 2\,Fe^{2+} + Ge^0 + 4\,I^- + 10\,CO$$
$$Mn_2(CO)_{10} + GeI_4 \rightarrow 2\,Mn^{2+} + Ge^0 + 4\,I^- + 10\,CO$$

In this convenient redox reaction, the formation of Fe^{+II}/Mn^{+II} and the crystallization of [BMIm][$M^{+II}(OTf)_3$] are obviously retarded, which favors crystal growth. The synthesis resulted in moisture-sensitive colorless and well-shaped needles of the title compounds. Crystals of [BMIm][$Li(OTf)_2$] were synthesized by direct heating of dried LiCl in [BMIm][OTf] and led also to the formation of moisture-sensitive, colorless and well-shaped needles. Interestingly, simple heating of $FeCl_2$ and $MnCl_2$ in [BMIm][OTf] – analogous to the reaction of LiCl in [BMIm][OTf] – only led to small, irregularly formed and conjoined crystals of [BMIm][$M(OTf)_3$] (M: Fe, Mn).

The chemical composition of all title compounds was verified, aside from X-ray structure analysis, by EDX, FT-IR and DTA-TG. Thus, EDX analysis evidences the presence of iron and manganese as well as of sulfur and fluorine for [BMIm][$M(OTf)_3$] (M: Fe, Mn). The measured metal-to-sulfur ratio of 1 : 2.8 ([BMIm][$Fe(OTf)_3$]) and 1 : 2.4 ([BMIm][$M(OTf)_3$]) matches within the significance of measurement with the expected ratio (1 : 3). For [BMIm][$Li(OTf)_2$], with lithium as a light element, EDX analyses is not meaningful. The presence of lithium was therefore verified *via* flame spectroscopy, indicating the red emission and the characteristic emission lines of lithium. FT-IR spectroscopy evidences the presence of the cation ($[BMIm]^+$) and the anion ($[OTf]^-$) (Fig. 1). Due to coordination of the oxygen atoms to the metal center, the S–O valence vibrations between 1300 and 1100 cm^{-1} are more expanded and slightly shifted to higher wavenumbers compared to the pure ionic liquid. According to TG analysis, all compounds show a one-step decomposition at temperatures of 320 – 350 °C. In addition, DTA exhibits weak endothermal peaks at 100 – 150 °C, indicating the melting points of the compounds (Table 1).

X-Ray structure analyses based on single crystals revealed [BMIm][$M(OTf)_3$] (M: Fe, Mn) to crystallize with monoclinic lattice symmetry and [BMIm][$Li(OTf)_2$] to crystallize in the triclinic space group $P\bar{1}$ (Table 2, Fig. 2). The compounds are composed of infinite $^1_\infty[M(OTf)_x]$ chains. Herein, the metal atoms are

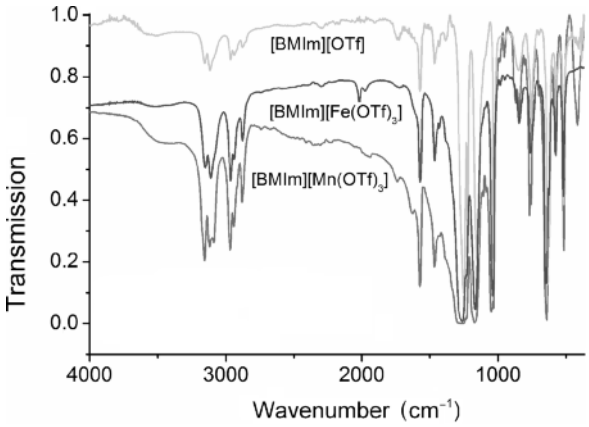

Fig. 1. FT-IR spectra of [BMIm][$M(OTf)_3$] (M: Fe, Mn) and of the pure ionic liquid [BMIm][OTf] as a reference.

Table 1. Melting points and decomposition temperatures of [BMIm][Fe(OTf)$_3$], [BMIm][Mn(OTf)$_3$] and [BMIm][Li(OTf)$_2$] as well as of the ionic liquid [BMIm][OTf] as a reference.

Compound	Melting point (°C)	Decomposition temperature (°C)
[BMIm][OTf]	−12	400
[BMIm][Li(OTf)$_2$]	98	300
[BMIm][Fe(OTf)$_3$]	142	360
[BMIm][Mn(OTf)$_3$]	153	350

interlinked by six (*M*: Fe, Mn) and four (*M*: Li) [OTf]$^-$ anions that act as bidentate bridging ligands (Figs. 3, 4). The infinite chains are oriented parallel to each other along the crystallographic *b* ([BMIm][*M*(OTf)$_3$] (*M*: Fe, Mn)) and *c* axis ([BMIm][Li(OTf)$_2$]). In all cases, the cations [BMIm]$^+$ are located between the one-dimensional *M*(OTf)$_x$ chains.

In [BMIm][*M*(OTf)$_3$] (*M*: Fe, Mn), each metal center is coordinated distorted octahedrally by six oxygen atoms from six different [OTf]$^-$ anions. The O–*M*–O angles range from 83.2(1) to 93.3(1)° for [BMIm][Fe(OTf)$_3$] and from 83.6(1)° to 95.9(2)° for [BMIm][Mn(OTf)$_3$]. The *trans*-angles deviate slightly from 180° with 174.9(1)–178.2(1)° for [BMIm][Fe(OTf)$_3$] and 174.6(1) – 178.2(1) for [BMIm][Mn(OTf)$_3$]. In [BMIm][Li(OTf)$_2$], the lithium atoms are coordinated in distorted tetrahedra. Compared to the tetrahedral reference angle of 109.5°, the angles are alternately widened and narrowed (104.9(2)–115.5(2)°). The *M*–O distances with 206.0(1) – 210.2(1) pm in [BMIm][Fe(OTf)$_3$] are slightly shorter than in [BMIm][Mn(OTf)$_3$] (212.1(1) – 215.6(1) pm), which correlates with the radii of the divalent cations (Fe^{2+}: 77 pm; Mn^{2+}: 80 pm [17]). In the case of [BMIm][Li(OTf)$_2$]), the Li-O distances – as expected – are much smaller (187.8(1) – 193.0(1) pm). With regard to known compounds that contain [OTf]$^-$ as a bidentate bridging ligand, the above *M*–O distances are comparably short (*e. g.* the mean Eu–O distance is 239.8 pm in [BMPyr]$_6$[Eu$_8$(μ_4-O)(μ_3-OH)$_{12}$(μ_2-OTf)$_{14}$(μ_1-Tf)$_2$](HOTf)$_{1.5}$) [8].

The parallel $^1_\infty$[*M*(OTf)$_x$] chains of all title compounds are interconnected *via* C–H···F hydrogen bonds between H atoms of the cations and fluorine atoms of the triflate anions. In the case of the Mn compound, three short hydrogen bonds are observed with distances around 263 pm (F3···H9A: 262.6(1); F6···H11A 262.7(1), F3···H11C: 264.0(1) pm), one

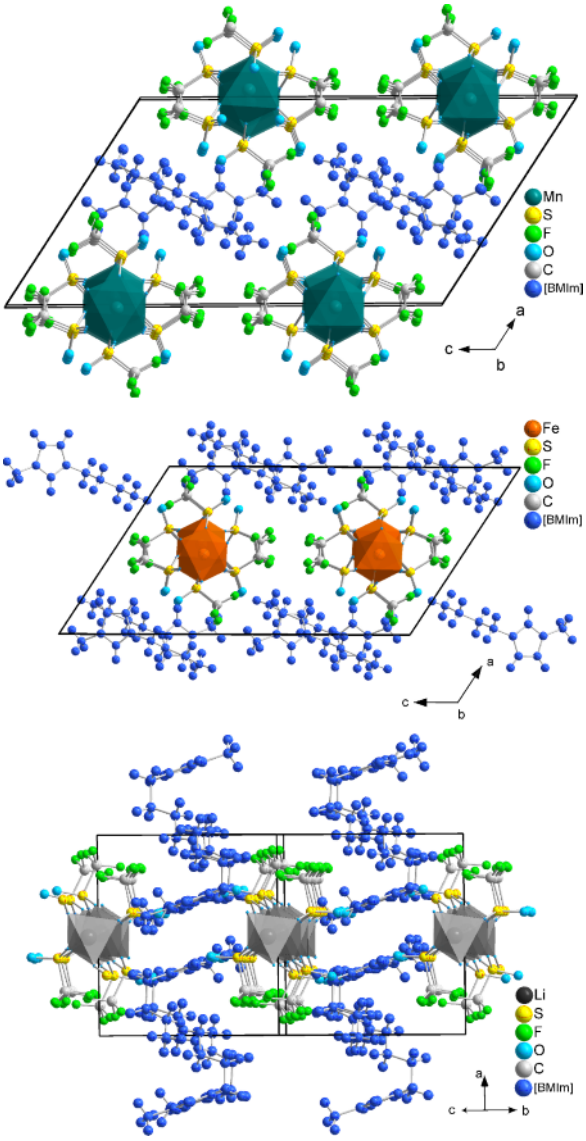

Fig. 2 (color online). Unit cells of [BMIm][Mn(OTf)$_3$] (top), [BMIm][Fe(OTf)$_3$] (middle) and [BMIm][Li(OTf)$_2$] (bottom).

with 269.8(1) pm (F7···H10B), and the longest ones with 274.6(1) (F4···H7B) and 287.1(1) pm (F4···H10A). The situation is similar for [BMIm][Fe(OTf)$_3$], however, the shortest hydrogen bond with 257.1(1) pm (F8···H11A) is even slightly shorter. For [BMIm][Li(OTf)$_2$], there are three hydrogen bonds of very different lengths. With 256.8(1), 263.0(1) and 263.3(1) pm, the shortest of these distances are observed for the Fe/Mn compounds. According to liter-

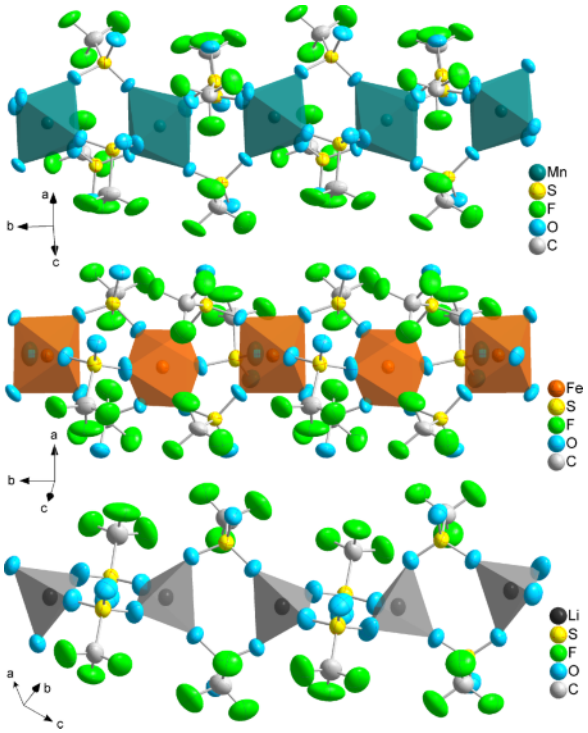

Fig. 3 (color online). Anionic one-dimensional coordination chains in [BMIm][Mn(OTf)$_3$] (top), [BMIm][Fe(OTf)$_3$] (middle) and [BMIm][Li(OTf)$_2$] (bottom) with the coordination polyhedra around Mn, Fe and Li. Cations have been omitted.

ature, all these values are in the range of moderate hydrogen bonding [18, 19].

The metal-to-metal distances in the chain-like [BMIm][M(OTf)$_3$] compounds are 463.3(1) (Fe···Fe) and 470.1(1) pm (Mn···Mn) (Figs. 3, 4), significantly exceeding the doubled covalent radii of 304 pm (Fe^{+II}) and 322 pm (Mn^{+II}) [17]. Consequently, any attractive metal-metal interaction can be excluded. The c axis in the manganese compound is slightly elongated as compared to the iron compound due to the larger radius of the Mn^{2+} cation. In view of the small size of Li^+ (59 pm) and due to its preferred tetrahedral coordination, the Li···Li distances in [BMIm][Li(OTf)$_2$] of 442.4(1) pm are much smaller as compared to [BMIm][M(OTf)$_3$] (M: Fe, Mn). Although the metal-to-metal distances are too long for any bonding interaction, for [BMIm][M(OTf)$_3$] (M: Fe, Mn) magnetic coupling might occur between the paramagnetic metal centers. To study such interactions, magnetic measurements of [BMIm][Fe(OTf)$_3$] were performed with a SQUID magnetometer (Fig. 5). Curie-Weiss behavior and strong antiferromagnetic coupling were observed, the experimental room temperature χT value being 3.04 cm^3 K mol^{-1}. These data are consistent with what is expected for high-spin Fe^{+II} ions (d^6, $S = 2$, $C = 3.0$ cm^3 K mol^{-1}). Since the preparation of phase-pure [BMIm][Mn(OTf)$_3$] turned out to be much more difficult than for the Fe compound, and since analogous antiferromagnetic coupling can be assumed for Mn^{2+} as well, magnetic measurements of [BMIm][Mn(OTf)$_3$] were not performed.

Conclusion

Ionic-liquid-based syntheses resulted in [BMIm][Fe(OTf)$_3$], [BMIm][Mn(OTf)$_3$] and [BMIm][Li(OTf)$_2$] as new coordination compounds that contain infinite [M(OTf)$_x$]$^-$ chains. Their bidentate bridging coordination by weakly coordinating [OTf]$^-$

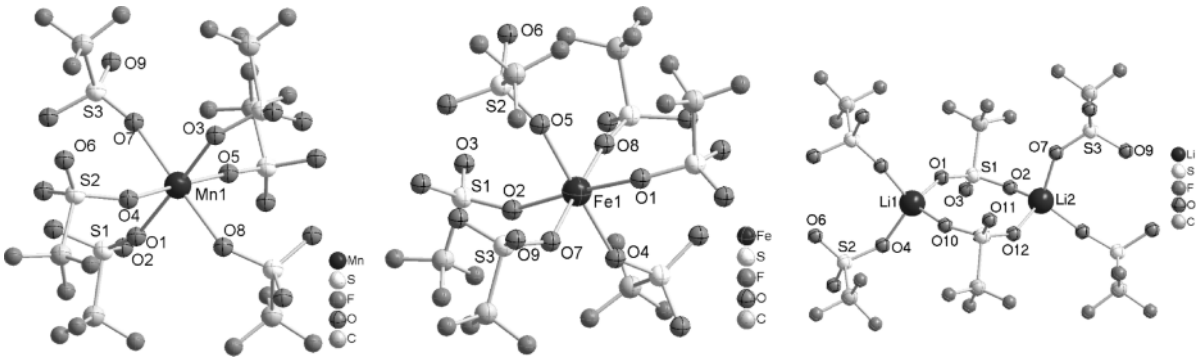

Fig. 4. Coordination of the metal centers in [BMIm][Mn(OTf)$_3$] (left), [BMIm][Fe(OTf)$_3$] (middle) and [BMIm][Li(OTf)$_2$] (right).

Table 2. Crystallographic data of [BMIm][Fe(OTf)$_3$], [BMIm][Mn(OTf)$_3$] and [BMIm][Li(OTf)$_2$].

Compound	[BMIm][Fe(OTf)$_3$]	[BMIm][Mn(OTf)$_3$]	[BMIm][Li(OTf)$_2$]
Empirical formula	$FeS_3F_9O_9N_2C_{11}H_{15}$	$MnS_3F_9O_9N_2C_{11}H_{15}$	$LiS_2F_6O_6N_2C_{10}H_{15}$
Formula weight	642.3 g mol^{-1}	641.4 g mol^{-1}	444.30 g mol^{-1}
Crystal system	monoclinic	monoclinic	triclinic
Space group	$P2_1/n$	$P2_1/c$	$P\bar{1}$
Lattice parameters	$a = 1294.3(3)$ pm	$a = 1293.3(3)$ pm	$a = 1120.0(2)$ pm
	$b = 917.8(2)$ pm	$b = 932.2(2)$ pm	$b = 1140.0(2)$ pm
	$c = 2262.4(5)$ pm	$c = 2281.3(5)$ pm	$c = 1530.0(3)$ pm
			$\alpha = 99.00(2)^\circ$
	$\beta = 123.14(3)^\circ$	$\beta = 123.23(3)^\circ$	$\beta = 103.40(3)^\circ$
			$\gamma = 99.01(3)^\circ$
	$V = 2250.4 \times 10^6$ pm^3	$V = 2300.6 \times 10^6$ pm^3	$V = 1836.8 \times 10^6$ pm^3
Formula units per cell, Z	4	4	4
Density (calculated)	1.90 g cm^{-3}	1.85 g cm^{-3}	1.61 g cm^{-3}
Absorption correction	numerical	numerical	numerical
Absorption coefficient	1.1 mm^{-1}	1.0 mm^{-1}	0.4 mm^{-1}
Measurement conditions	Image plate diffractometer IPDS II (STOE) λ(Mo K_α) = 71.073 pm; T = 200 K		
Measurement limits	$-17 \le h < 17$; $-10 \le k \le 12$; $-31 \le l \le 31$; $2\theta_{max} = 58.70^\circ$	$-17 \le h < 17$; $-12 \le k \le 0$; $-16 \le l \le 31$; $2\theta_{max} = 58.47^\circ$	$-15 \le h < 13$; $-15 \le k \le 13$; $-20 \le l \le 20$; $2\theta_{max} = 58.57^\circ$
Number of reflections	8884 (independent 6096)	17 988 (independent 16 189)	21 332 (independent 17 946)
Merging	$R_{int} = 0.068$	$R_{int} = 0.050$	$R_{int} = 0.055$
Refinement method	Full-matrix least-squares on F^2		
Total number of least squares parameters	319	318	491
Figures of merit	$R1 = 0.053$ [3926 $F_o > 4\,\sigma(F_o)$]	$R1 = 0.037$ [1747$F_o > 4\,\sigma(F_o)$]	$R1 = 0.055$ [9152 $F_o > 4\,\sigma(F_o)$]
	$R1$ (all data) = 0.163	$R1$ (all data) = 0.166	$R1$ (all data) = 0.0864
	$wR2 = 0.130$	$wR2 = 0.078$	$wR2 = 0.164$
	GooF = 0.816	GooF = 0.511	GooF = 1.029
Largest diff. peak / hole	0.49 / −0.77 e$^-$ × 10^{-6} pm^3	0.29 / −0.34 e$^-$ × 10^{-6} pm^3	0.54 / −0.45 e$^-$ × 10^{-6} pm^3

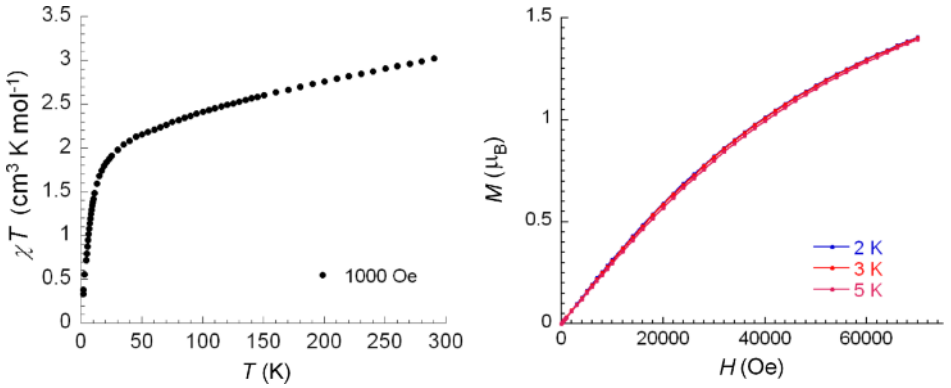

Fig. 5 (color online). Magnetic properties of [BMIm][Fe(OTf)$_3$].

anions is still rare. Although [BMIm][Fe(OTf)$_3$] and [BMIm][Mn(OTf)$_3$] can be obtained by simple heating of $FeCl_2$ and $MnCl_2$ in [BMIm][OTf], a significantly improved crystal quality is achieved by applying the mild oxidation of $Fe(CO)_5$/$Mn_2(CO)_{10}$ by GeI_4 in the ionic liquids. The decelerated formation of [BMIm][Fe(OTf)$_3$] and [BMIm][Mn(OTf)$_3$] favors a controlled crystal growth in the highly viscous ionic liquid. Crystal structure and phase composition of all title compounds were validated by crystal structure analysis, EDX, FT-IR and DTA-TG. DTA indicates a melting of the title compounds in the range 98 – 150 °C and the thermal decomposition at 300 – 350 °C. Magnetic measurements show Curie-Weiss behavior with strong antiferromagnetic coupling for [BMIm][Fe(OTf)$_3$].

Experimental Section

General considerations

All sample handling was carried out under standard Schlenk and argon glove-box techniques. Reactions took place in argon-filled and sealed glass ampoules that were dried under reduced pressure (1×10^{-3} mbar) at 300 °C before use. The commercially available starting materials $FeCl_2$ (98 %, Sigma Aldrich), $MnCl_2$ (> 99 %, Sigma Aldrich) and LiCl (> 99 %, Aldrich) were dried overnight by heating to 150 °C in vacuum; $Fe(CO)_5$ (99.999 %, Sigma Aldrich), $Mn_2(CO)_{10}$ (98 %, Sigma Aldrich) and GeI_4 (99.99 % Sigma Aldrich) were used as received. The ionic liquid [BMIm][OTf] (Merck, 99 %) was dried under vacuum at 100 °C for 48 h before use.

Syntheses

[BMIm][Fe(OTf)$_3$]

$FeCl_2$ (100 mg) was dissolved in the ionic liquid [BMIm][OTf] (1 mL) and heated in a sealed glass ampoule at 130 °C for 4 d. After cooling to room temperature with a rate of 1 K h^{-1}, very small and conjoined colorless crystals of limited quality were obtained. Well-shaped transparent crystals were alternatively obtained by reacting $Fe(CO)_5$ (0.02 mL, 0.15 mmol) and GeI_4 (100 mg, 0.17 mmol) in the ionic liquid [BMIm][OTf]. This solution was left in a sealed glass ampoule at 130 °C for 10 days. After cooling to room temperature with a rate of 1 K h^{-1}, well-shaped colorless, transparent crystals were obtained in large quantities (about 70 % yield according the total amount of iron). In addition, a dark-grey residue was observed that according to X-ray diffraction analysis turned out to be elemental germanium. Crystals of the title compound were separated manually for crystal structure analysis.

[BMIm][Mn(OTf)$_3$]

[BMIm][$Mn(OTf)_3$] was synthesized similarly. Instead of $FeCl_2$, $MnCl_2$ was used. For high-quality crystals, $Mn_2(CO)_{10}$ (48 mg, 0.12 mmol) was reacted with GeI_4 (100 mg, 0.17 mmol) in 1 mL ionic liquid. The compound crystallizes as colorless, transparent needles, but, in contrast to [BMIm][$Fe(OTf)_3$], with limited yield of only about 10 %.

Analytical tools

Crystal structure determination

Single-crystal structure analyses of all title compounds were performed on an IPDS II diffractometer (Stoe, Darmstadt) using graphite-monochromatized MoK_α radiation ($\lambda = 71.073$ pm). Suitable crystals were isolated in inert oil and mounted on a glass capillary. Structure solution and refinement were conducted based on the program package SHELX [20]. The results are listed in Table 2. A numerical absorption correction was applied; hydrogen atoms were geometrically constructed [20]. All illustrations were created with DIAMOND [21].

CCDC 900307 ([BMIm][$Fe(OTf)_3$]), CCDC 900309 ([BMIm][$Mn(OTf)_3$]) and CCDC 900308 ([BMIm][$Li(OTf)_2$]) contain the supplementary crystallographic data for this paper. These data can be obtained free of charge from The Cambridge Crystallographic Data Centre *via* www.ccdc.cam.ac.uk/data_request/cif.

Energy-dispersive X-ray analysis

EDX was carried out using an AMETEC EDAX device mounted on a Zeiss SEM Supra 35 VP scanning electron microscope. For measurement, single crystals were fixed with conductive carbon pads on aluminum sample holders.

Fourier-transformed infrared spectroscopy

FT-IR spectra were recorded on a Bruker Vertex 70 FT-IR spectrometer; the samples were measured as pellets in KBr. For this purpose, 300 mg of dried KBr and 2 mg of the sample were carefully pestled together and pressed to a thin pellet.

Differential thermal analysis/thermogravimetry

DTA/TG were performed with a Netzsch STA 409C instrument applying α-Al_2O_3 as a crucible material and reference sample. The samples were heated under N_2 flow to 800 °C with a heating rate of 5 K min^{-1}.

Magnetic measurements

Magnetic measurements were performed with a Quantum Design MPMS-XL SQUID magnetometer using samples composed of single crystals at temperatures between 1.8 and 300 K with magnetic fields up to 7 T. The susceptibility was measured with 1000 Hz and 3 Oe oscillating alternating magnetic field (1 Oe = 79.6 A m^{-1}). Corrections for sample holder and diamagnetic contribution were applied.

Acknowledgement

The authors are grateful to the Center for Functional Nanostructures (CFN) of the Deutsche Forschungsgemeinschaft (DFG) at the Karlsruhe Institute of Technology (KIT) for financial support.

[1] P. Wasserscheid, T. Welton, *Ionic Liquids in Synthesis*, Wiley-VCH, Weinheim **2008**.
[2] R. E. Morris, *Angew. Chem. Int. Ed.* **2008**, *47*, 442 (review).
[3] R. Giernoth, *Angew. Chem. Int. Ed.* **2010**, *49*, 2834 (review).
[4] M. Antonietti, D. Kuang, B. Smarsly, Y. Zhou, *Angew. Chem. Int. Ed.* **2004**, *43*, 4988 (review).
[5] D. Freudenmann, S. Wolf, M. Wolff, C. Feldmann, *Angew. Chem. Int. Ed.* **2011**, *50*, 11050 (review).
[6] E. Ahmed, M. Ruck, *Dalton Trans.* **2011**, *40*, 9347 (review).
[7] E. Boros, M. J. Earle, M. A. Gilea, A. Metlen, A.-V. Mudring, F. Rieger, A. J. Robertson, K. R. Seddon, A. A. Tomaszowska, L. Trusov, J. S. Vyle, *Chem. Commun.* **2010**, *46*, 716.
[8] A. Babai, A.-V. Mudring, *Z. Anorg. Allg. Chem.* **2006**, *632*, 1956.
[9] A. Babai, A.-V. Mudring, *Inorg. Chem.* **2006**, *45*, 3249.
[10] P. Nockemann, B. Thijis, K. Van Hecke, L. Van Meervelt, K. Binnemans, *Cryst. Growth Des.* **2008**, *8*, 1354.
[11] G. Korus, M. Jansen, *Z. Naturforsch.* **1998**, *42b*, 438.
[12] F. Charbonnier, R. Faure, H. Loiseleur, *Acta Crystallogr.* **1977**, *B33*, 1478.
[13] R. Faure, H. Loiseleur, F. Charbonnier, *Acta Crystallogr.* **1977**, *B33*, 2824.
[14] C. Rim, H. M. Zhang, D.-Y. Son, *Inorg. Chem.* **2008**, *47*, 11993.
[15] M. Wolff, J. Meyer, C. Feldmann, *Angew. Chem. Int. Ed.* **2011**, *50*, 4970.
[16] S. Wolf, C. Feldmann, *Dalton Trans.* **2012**, *41*, 8455.
[17] A. F. Holleman, E. Wiberg, N. Wiberg, *Lehrbuch der Anorganischen Chemie*, 102nd ed., de Gruyter, Berlin **2007**.
[18] T. Steiner, *Angew. Chem. Int. Ed.* **2002**, *41*, 48.
[19] G. A. Jeffrey, *An Introduction to Hydrogen Bonding*, Oxford University Press, Oxford **1997**.
[20] G. M. Sheldrick, *Acta Crystallogr.* **2008**, *A64*, 112.
[21] K. Brandenburg, DIAMOND (version 3.1d), Crystal and Molecular Structure Visualization, Crystal Impact – K. Brandenburg & H. Putz GbR, Bonn (Germany) **2005**. See also: http://www.crystalimpact.com/diamond/.